Available online at www.sciencedirect.com

ScienceDirect

journal homepage: www.elsevier.com/locate/jtte

Original Research Paper

Estimation of vehicle queuing lengths at metering roundabouts

Hong Ki An [a,*], *Wen Long Yue* [a], *Branko Stazic* [b]

[a] *School of Natural and Built Environments, University of South Australia, Adelaide, SA 5001, Australia*
[b] *School of Computer Science, Engineering and Mathematics, Flinders University, Clovelly Park, SA 5042, Australia*

HIGHLIGHTS

- The inventive numerical model developed for queuing length estimation can predict queuing length on each approach at a metering roundabout.
- The numerical model can define the relationships between queuing length, detector location and signal phase time.
- The popular microscopic simulation model, AIMSUN, was introduced and used for network modeling and calibration methods applicable to metering roundabouts.

ARTICLE INFO

Article history:
Received 28 November 2016
Received in revised form
26 April 2017
Accepted 27 April 2017
Available online 11 November 2017

Keywords:
Unbalanced traffic flow
Metering roundabout
Advance detector location
AIMSUN
Queuing length estimation model

ABSTRACT

Signalized metering roundabouts are equipped with advanced loop detectors and traffic signals that can reduce vehicle queuing lengths, especially on the dominant approach, when unbalanced traffic flow conditions occur. At a metering roundabout, changeable queuing lengths and the location of detectors determine signal phase times, which in turn affect queuing length on each approach. To date, most studies have focused on performance comparisons between normal and metered roundabouts, but have failed to evaluate the effect of detector locations on queuing formations. In addition, no guidelines have been developed to enable practitioners to select the appropriate detector location that would lead to optimum roundabout performance. This study, therefore, formulated a numerical model for the estimation of queuing length at a metering roundabout. The model consists of advance vehicle detectors on two approaches and one traffic signal. In order to calibrate and verify the model, queuing lengths were recorded using two drones for the Old Belair Road metering roundabout in Adelaide, South Australia. In order to assess the fitness of the model, an R^2 test was conducted, and the results showed that the numerical model can predict queuing lengths on the controlling and metered approaches with up to 83% of R^2 value. Moreover, the estimated queuing lengths were compared against those predicted by the software AIMSUN for the same location and under the same conditions. It is expected

* *Corresponding author*. Tel.: +61 8 8302 1120.
E-mail addresses: hong_ki.an@mymail.unisa.edu.au (H. K. An), wen.yue@unisa.edu.au (W. L. Yue), branko.stazic@flinders.edu.au (B. Stazic).

Peer review under responsibility of Periodical Offices of Chang'an University.
https://doi.org/10.1016/j.jtte.2017.04.002

that the model will assist and guide practitioners in determining the best detector locations for metering roundabouts.

1. Introduction

Metering roundabouts controlled by advanced detectors and traffic signals are rare, but operated in some countries including Australia. The main purpose of a metering roundabout is to reduce the concentrated queuing length on a dominant approach during peak time periods (Martin-Gasulla et al., 2016a; Robinson et al., 2000; Sides, 2000), and it can also be one of the solutions when there are unbalanced traffic flow conditions (Akçelik, 2004, 2006, 2011; Azhar and Svante, 2011; Hummer et al., 2014; Krogscheepers and Roebuck, 2000).

Basically, a metering roundabout is operated by detectors and traffic signals in accordance with queuing length. Fig. 1 illustrates the operational concept of a metering roundabout that is composed of two detectors; Detector C is on the dominant (controlling) approach and Detector M is on the sub-dominant (metered) approach, with one traffic signal on the metered approach. Its operation principle is that when the queuing length on the controlling approach reaches Detector C's position, the signal changes to red. Additionally, if Detector M on the metered approach detects the queuing, the red signal dissipates. Therefore, the location of the detectors on a metering roundabout is a crucial element that affects the signal red times, which will consequently affect queuing lengths on the controlling, metered and other approaches.

In recent years, a number of researchers have conducted performance analyses between normal roundabouts and metering roundabouts using traffic modeling software. Although some researchers have attempted to estimate the queuing length for metering roundabouts, a standard has not been defined. The lack of a standard is due to the determination of the relationship between queuing length and signal time split, as it is a difficult task for changeable vehicle queuing lengths in real time.

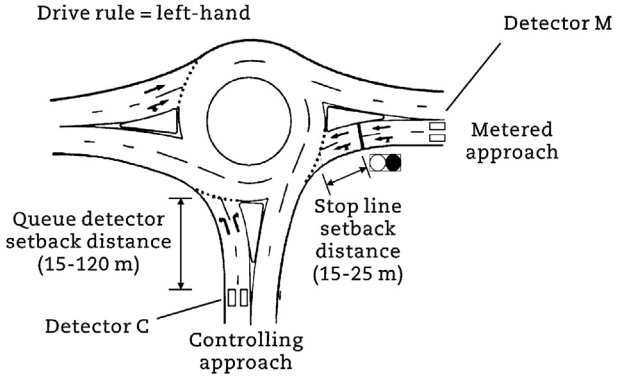

Fig. 1 – Concept of metering roundabout (modified from Akçelik (2011)).

Therefore, this study developed a numerical model for the estimation of queuing lengths on the controlling, metered and other approaches. Model calibration and verification were conducted using real-life data recorded collected by two drones, and the predicted queuing lengths were then regenerated using AIMSUN 7 based on the Old Belair Road metering roundabout in Adelaide, South Australia. Traditionally, fixed video camera scan be used for dynamic traffic data recordings in traffic engineering cases; due to the limited visibility and large queuing extensions, however, in this study two drones were applied for more accurate data collections. In addition, a comparative study between the developed model and AIMSUN 7 simulation was conducted. This software is a widely used tool in traffic engineering studies that is capable of simulating roundabouts with multiple advanced detectors and allows easy detector location re-positioning.

2. Literature review

As mentioned earlier, majority of studies on metering roundabouts have concentrated on performance analyses using existing software. In addition, fixed video cameras have usually been used for data collection, including critical gaps, modeling of traffic flows and driver behavior analyses, as conducted by Luttrell et al. (2000), Mensah et al. (2010) and Xu and Tian (2008). Although fixed video cameras are sufficient to observe vehicle movements in specific areas, they are not able to record long vehicle queues from all approaches.

Numerous studies related to metering roundabouts have been undertaken by many researchers over the past decade or so. However, the analyses of the effect when a normal roundabout converts to a metering roundabout using software make up the majority. Little has been commented on detector location related issues.

Akçelik (2005) analyzed metering roundabouts considering approach capacity, average delay time, queuing length and CO_2 emissions based on Mickleham Road and Broadmeadows Road roundabout in Melbourne, Australia, using SIDRA software. His conclusions showed that metering signals reduced average delay time, queuing length and CO_2 emissions when compared to a normal roundabout. In addition, Stevens (2005) claimed that metering signals can enhance roundabout performance. However, he indicated that more studies were required, for example, choice of control (entering vehicles/circulating vehicles/entering + circulating), choice of signal operation (full time/part time), and choice of

approaches (all approaches/one or two approaches) to be signalized, but failed to provide any solutions.

Akçelik (2006) conducted another case study, based on the Nepean Highway and McDonald Street in Melbourne, Australia. He analyzed the performance of the roundabout in accordance with five scenarios related to signal time using the analytical model SIDRA. He found that metering signals can reduce delays and queues. He further argued that metering signals can be successfully deployed in situations with unbalanced traffic flows. However, SIDRA is a static analytical model, it might not be capable to respond to situations, such as variation of approach flows and when signal to be applied.

Vlahos et al. (2008) also investigated the effectiveness of metering roundabouts compared with all-way-stop-intersections using SIDRA 2.1 software. A different entry turning ratio was applied on the major approach at two single-lane roundabouts in Maryland (MD) near Delaware, US. The estimated critical gaps were considered to be 3.85 s for the MD 273/MD 276 roundabout, and 3.91 s for the MD 18/Castle Marina Road roundabout for capacity, delays and queues. The researcher concludes that if the vehicle entry volume is less than 2400 vph, the metering roundabout has an advantage in the order of 190% of capacity enhancement, and a decrease of 49% in delay and 41% in queuing length.

Geers et al. (2009) conducted a study for a metering roundabout with the aim of analyzing delay time at the Yallah roundabout in Sydney, Australia, which had unbalanced traffic flow conditions during AM and PM peak times. Field data, such as queuing length on each approach, was observed by video cameras. The delay time of the roundabout was derived using a microscopic simulation model built in PARAMICS software. The results showed that the use of metering can decrease delay time significantly when compared with non-metering. This is because red time provides enough gap times to entering vehicles on a dominant approach.

Hummer et al. (2014), provided the guidance on the use of metering signals. Their study involved simulations using VISSIM software. Moreover, they stated that a roundabout with metering signals is helpful when there are unbalanced traffic conditions during peak times.

A comparison study between signal roundabouts and signal intersections was conducted by Sun et al. (2016). In their research, a shockwave based model was applied and its sensitivity analysis was tested. The study concluded that if features of geometry are similar, signalized roundabouts have larger capacity than signalized intersections.

A recent study by Afezolli and Shehu (2016) undertook a capacity comparison between a normal and metering roundabout using SIDRA. The Shqiponja roundabout in Albania was used in their study as it was experiencing congestion problems due to unbalanced traffic conditions. Three analysis methods without metering, metering operation and signalized intersection-were compared for measurement of queuing length on the controlling and metered approaches. As expected, when the roundabout was controlled by the metering operation, 20%–40% of queuing length on the controlling approach was reduced.

Martin-Gasulla et al. (2016a,b) analyzed capacity effect based on a 5-leg with single lane metering roundabout in Valencia, Spain. VISSIM was used for comparison capacity analysis between metered and unmetered roundabouts. The authors found that a metering system can generate a platoon on the metered approach providing a longer acceptable gap. Thus, the capacity of the selected metering roundabout is doubled when the conflicting volume is at 1200 vph level.

However, Afezolli and Shehu (2016), Geers et al. (2009), Hummer et al. (2014), Martin-Gasulla et al. (2016a,b), Sun et al. (2016) and Vlahos et al. (2008), failed to consider how detector locations and signal settings will affect the performance of metering roundabouts.

Few studies have tried to define unbalanced traffic flow conditions. One, conducted by Krogscheepers and Roebuck (2000), stated that an unbalanced traffic condition can be generated by the circulating traffic because vehicle movements at the roundabout are complex and not individual, as at T-junctions. Thus, they developed a formula defining unbalanced flows, where the value of ρ_s equals 0 represents unbalanced flow due to a second upstream approach, 0.5 represents balanced flow, and 1 represents unbalanced flow due to the first upstream approach as described in Eq. (1) and Fig. 2.

$$\rho_s = \frac{Q_{ws}}{Q_{ws} + Q_{ns} + Q_{es}} = \frac{Q_{ws}}{Q_{sc}} \quad (1)$$

where ρ_s is the proportion of the ratio of unbalanced flow for the southern approach, Q_{ws} is traffic from the western approach passing the southern approach, Q_{ns} is traffic from the northern approach passing the southern approach, Q_{es} is traffic from the eastern approach passing the southern approach, Q_{sc} is traffic passing southern, that might conflict over traffic from southern approach as shown in Fig. 2.

In terms of detector locations, Koonce et al. (2002), Liu et al. (2004), Oh and Choi (2004), and Zhou et al. (2006) attempted to find the optimal detector location for a bus transit priority at signalized roundabouts. However, an application of the

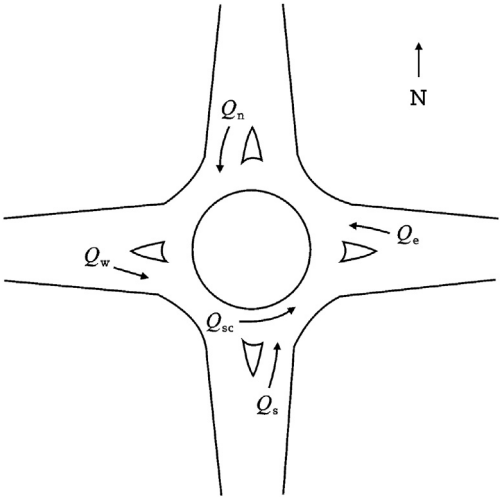

Fig. 2 – Definition of unbalanced conditions (Chapman and Benekohal, 2002).

detector location, which is derived from the signalized intersections, at the metering roundabout is fallacious due to the different operating principles. Vehicle movements at signalized intersections are decided by signal phase sequences, and turning movement behaviors are different from which at roundabouts. Thus, the location of detectors, circulating traffic, signal phase durations and entry traffic should be taken into account in the queuing length or detector location estimation model for the optimization of roundabout performance.

The following section elucidates the methodology in order to demonstrate how the numerical model can be developed, calibrated and verified.

3. Research methods

As discussed in Section 2, there was no comprehensive study that explained how roundabout detector location relates to queuing length, circulating traffic and signal phase time durations. Thus, in order to estimate the queuing length based on detector locations and signal phase times, this study formulated a numerical model with six main parameters that significantly affect the formation of queuing length. Based on drone recordings, model calibration and verification were conducted, then microscopic simulation model AIMSUN 7, was employed to evaluate the queuing lengths for various detector location changes. In order to deal with the stochastic nature of modeling, 10 replications were conducted in the simulation process in each scenario and their average queuing length was further analyzed. The procedures are presented in Fig. 3.

3.1. *Numerical model development*

Entry capacity and critical gap times at roundabouts are related to circulating traffic volumes (Akçelik et al., 1996; Flannery et al., 2005; Guo, 2010; Silva et al., 2013; Waddell, 1997). Consequently, the queuing length on each approach is affected by the circulating traffic volumes. Therefore, a queuing estimation model should include the relationship between queuing length and circulating volumes. As shown in Fig. 4, the queuing length at a metering roundabout can be affected by other factors, such as detector location, vehicle presence time on the detectors and signal phase time.

Signal split time on the metered approach, traffic volume on the controlling approach, conflict volume against the controlling approach, detector location on the controlling approach and vehicle presence time on the controlling approach detector are the parameters that are directly proportional to queuing length on the controlling approach. On the other hand, detector location on the metered approach and its vehicle presence time are inversely proportional. In the model, location of two detectors (Detectors C and M), which have an indirect relationship, contributes to the queuing length result. Therefore, the queuing length estimation model for the controlling approach can be expressed as follow

$$Q_{con} = \frac{\frac{P_{nor}}{T}\frac{\frac{V_i}{N_L}}{T} \times \frac{\frac{V_{ci}}{N_L}}{T} \times DL_C PT_C VS}{DL_M PT_M}\alpha \quad (2)$$

where Q_{con} is the queuing length of the controlling approach, P_{nor} is the normal time (s), N_L is the number of lane, V_i is the arrival volume of subject i approach (vehs), V_{ci} is the conflict volume against subject i approach, DL_C is the detector location on the controlling approach (km), DL_M is the detector location on the metered approach (km), VS is the vehicle space (m), PT_C is the vehicle presence time on the Detector C (s), PT_M is the vehicle presence time on the Detector M (s), α is the calibration constant for controlling approach, T is time.

Moreover, the queuing length on the metered approach has a proportional relation to signal red time on the metered approach, arrival volume on the metered approach, conflict volume against metered approach and detector location on the metered approach and its vehicle presence time, whereas detector location on the controlling approach and its vehicle presence time have an inverse proportion in relation to the queuing length on the metered approach as follow

$$Q_{met} = \frac{\frac{P_{red}}{T}\frac{\frac{V_i}{N_L}}{T} \times \frac{\frac{V_{ci}}{N_L}}{T} \times DL_M PT_M VS}{DL_C PT_C}\beta \quad (3)$$

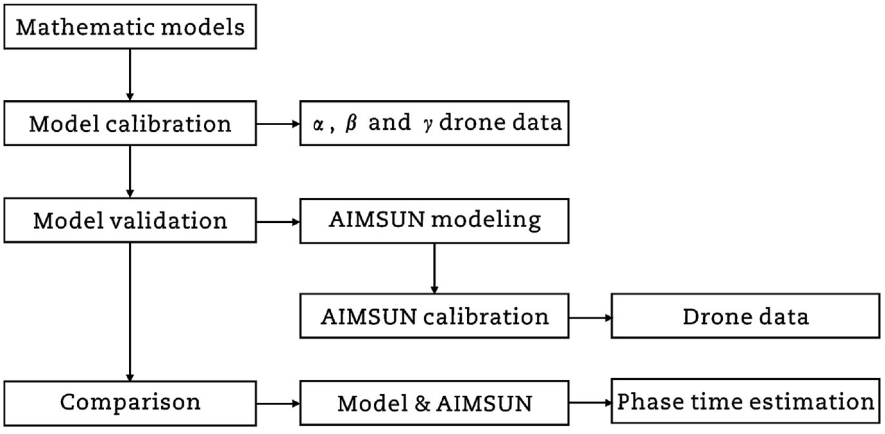

Fig. 3 – Research flowchart.

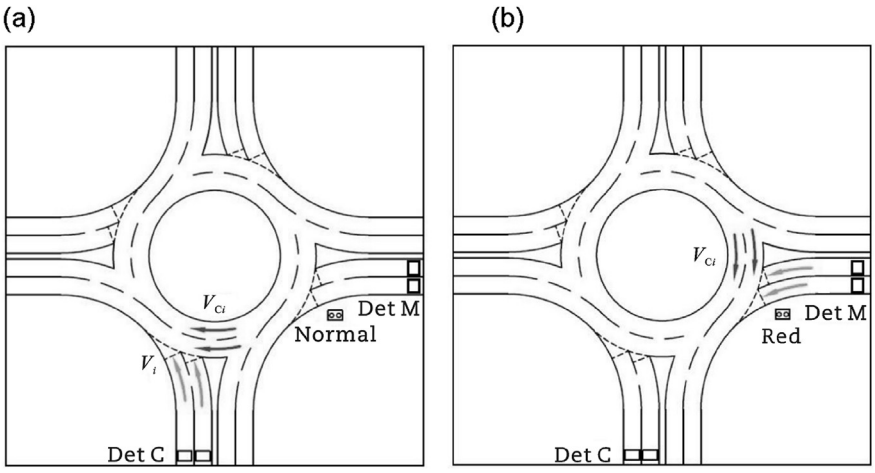

Fig. 4 – Effective parameters for queuing length. (a) Controlling approach. (b) Metered approach.

where Q_{met} is the queuing length of the metered approach, P_{red} is the red time (s), β is the calibration constant for metered approach.

For queuing length on the other approaches Q_o, the formula below, similar to the controlling approach, is applied. The applied parameters are the same as the queuing length model on the controlling approach. However, a different calibration constant (γ) needs to be considered.

$$Q_o = \frac{\frac{P_{nor}}{T}\frac{\frac{V_i}{N_L}}{T} \times \frac{\frac{V_{ci}}{N_L}}{T} \times DL_C PT_C VS}{DL_M PT_M}\gamma \quad (4)$$

3.2. *Model calibration and the determination of α, β and γ values*

In order to conduct model calibration, and determine the values of α, β and γ, data collection using two drones was conducted at the Old Belair Road roundabout in Adelaide, South Australia. The roundabout is operated by two sets of advance detectors and one traffic signal during PM peak (17:10–17:55).

3.2.1. *Data collection*

Among the six main parameters which affect queuing length on each approach, arrival volume, conflict volume and phase time values were extracted from Sydney Coordinated Adaptive Traffic System (SCATS). In addition, vehicle presence time on each detector was adopted, as used by the South Australian Department of Planning, Transport and Infrastructure (DPTI) for the Old Belair Road roundabout.

Thus for vehicle presence time, 3 s for the controlling approach detector and 4 s for the metered approach were applied. In addition, the queuing length on each approach was recorded by two drones at the same time, and the areas covered as shown in Fig. 5. The drones can record for a maximum 25 min with one battery, and are equipped with a hovering function that is useful for chasing the back of queues. Furthermore, a high definition (HD) camera is also set up on the bottom of the main drone to identify the vehicle clearly.

Since the Australian law allows only non-commercial drone to fly below 120 m in height, and it can move only vertically, Drone 1 was used to observe the queuing length on the northern approach where the maximum queuing length is longer, and Drone 2 captured the queuing length for the other three approaches. The drone launch sites were all open spaces and there were no vertical obstructions.

3.2.2. *Data results*

Table 1 shows the results of the main parameters that is used in queuing length model on each approach collected using the drones and from SCATS. Although the cycle time of the Old Belair Road roundabout is 120 s, 5-min time intervals (300 s) were set because a minimum interval of 5 min for the values of the arrival volume (V_i) and conflict volume (V_{ci}) could be extracted from the SCATS data.

Table 2 presents the maximum queuing length on each approach as observed by the drones and calculated by the formulated models. The calibration constants of α, β and γ were found to be 2930, 9000 and 1050 respectively. When the constants were applied, apart from the eastern approach, the R^2 value of each approach was higher than 0.83, and also the sum of each time period queuing length appeared very similar (i.e., northern approach drone: 7080 m, northern approach model: 7070 m). In addition, the vehicle space length of 7 m was applied as recommended by Akçelik (2010). The final queuing lengths are shown in the table below.

The queuing length of the southern and eastern approaches were less than 50 m during the survey periods, and total queuing length in 45 min was also less than 300 m, as shown in Fig. 6. This study only considered two main approaches, western and northern, as queuing lengths are most significant in these approaches.

In terms of the queuing length pattern, the queuing length on the western (metered) approach increased as the time increased. However, the queuing length on the northern (controlling) approach fluctuated.

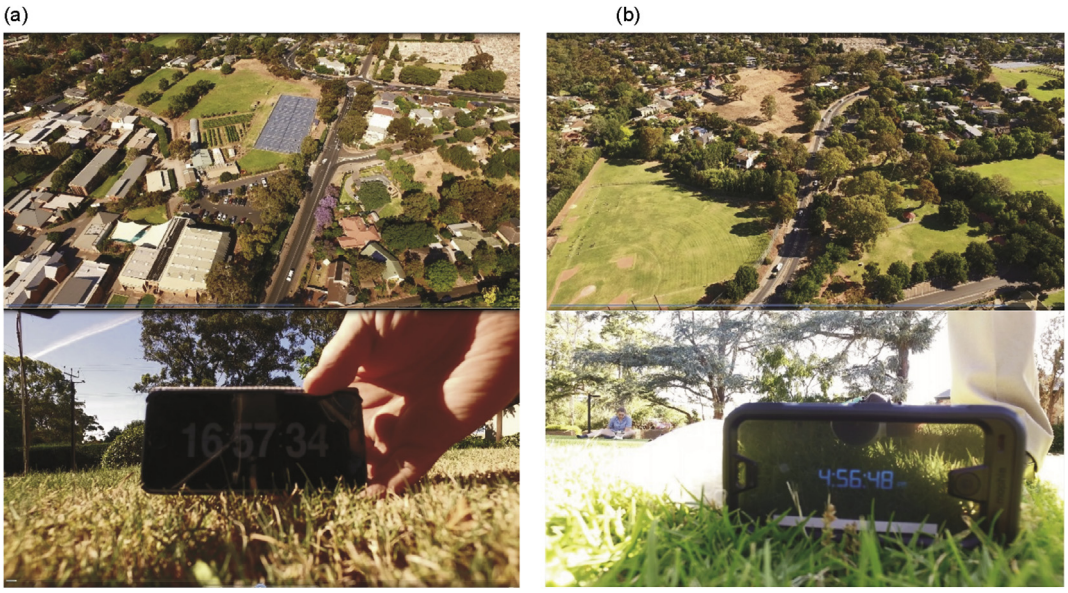

Fig. 5 – Drone footage and time stamp. (a) Drone 1. (b) Drone 2.

Table 1 – Parameter values.

Time	Vehicle								Phase (s)		
	Southern		Western		Northern		Eastern				
	V_s	V_{cs}	V_w	V_{cw}	V_n	V_{cn}	V_e	V_{ce}	Normal	Red	Total
17:10–17:15	20	41	97	18	108	52	5	145	207.0	93.0	300
17:15–17:20	24	57	77	20	95	42	4	160	210.0	90.0	300
17:20–17:25	22	49	89	23	128	44	5	162	205.5	94.5	300
17:25–17:30	18	34	97	22	114	57	0	143	196.0	104.0	300
17:30–17:35	23	33	69	27	84	47	2	125	193.5	106.5	300
17:35–17:40	29	46	79	36	76	43	4	125	202.0	98.0	300
17:40–17:45	26	55	81	33	106	44	2	156	202.5	97.5	300
17:45–17:50	36	58	71	37	128	38	3	171	194.0	106.0	300
17:50–17:55	27	51	87	36	131	47	0	161	195.0	105.0	300

Table 2 – Queuing length on each approach.

Time	Southern		Western		Northern		Eastern	
	Drone (m)	Model (m)	Drone (m)	Model (m)	Drone (m)	Model (m)	Drone (m)	Model (m)
17:10–17:15	15	25	152	183	770	926	10	22
17:15–17:20	40	43	210	158	720	657	15	20
17:20–17:25	30	33	235	221	880	907	15	25
17:25–17:30	15	18	228	251	1000	1007	0	0
17:30–17:35	20	22	220	226	700	606	7	7
17:35–17:40	45	40	302	313	580	519	7	15
17:40–17:45	40	43	310	293	730	743	10	9
17:45–17:50	50	60	330	310	750	755	7	15
17:50–17:55	30	40	335	368	950	950	0	0
Total	290	324	2297	2323	7080	7070	71	113
R^2	0.8617		0.8300		0.8404		0.7829	

3.3. *Model verification*

In order to verify the developed numerical model, this study compared vehicle queuing lengths with those generated by the microscopic simulation software AIMSUN 7, used widely for intersection analysis.

3.3.1. *AIMSUN modeling*

An AIMSUN model (Fig. 7) was developed to replicate the Old Belair Road roundabout operation accurately. The model had two sets of detectors and its traffic signal phase settings matched real-life conditions. Detector C was located at 305 m from the stop line on the northern approach

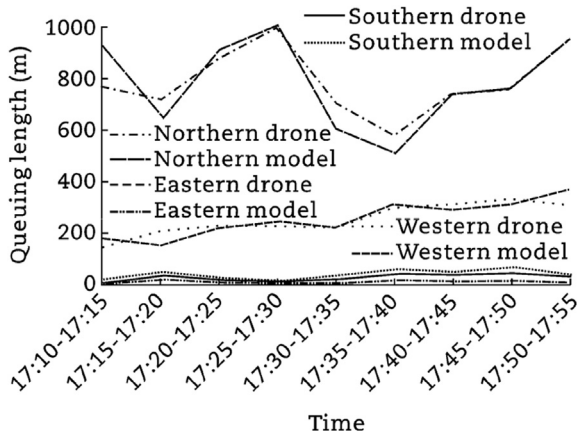

Fig. 6 – Queuing length: drones vs models.

(controlling approach), and Detector M at 220 m from the stop line. The traffic signals were installed on the western (metered) approach.

The arrival volumes (SCATS data) and vehicle turning ratios (drone data) for 45 min were specified as model traffic demand data (Tables 1 and 3). The feature of volume patterns is that the majority of vehicles from the southern approach exited towards the northern approach. Moreover, around 71% of vehicles from the northern approach passed through the southern exit approach.

3.3.2. *AIMSUN calibration and results*

In order to achieve successful AIMSUN model calibration and match queuing length with drone data, yellow-box speed, exit speed, visibility distance and vehicle presence time on the detectors needed to be adjusted. Yellow-box speed is a unique function in AIMSUN that deals with vehicle departures from roundabouts. Vehicles entering the roundabout have to avoid conflict with vehicles already in the roundabout. Thus, approaching vehicles enter the roundabout when the preceding vehicle is below yellow-box speed. The yellow box speed can be described as the vehicle speed on the circulating lane, and speeds of 17 km/h (northern), 15 km/h (eastern), 15 km/h (southern) and 14 km/h (western) were applied. The presence time can be described as a time that vehicles occupy the detectors, thus the value of 66.8% (northern) and 72.5% (western) in occupancy were used. In addition, the visibility speed represents the distance that vehicles are able to observe the feasible turning point, and 10 m of visibility distance was applied, apart from the western approach (Table 4).

Fig. 7 – Old Belair Road roundabout in AIMSUN 7.

Table 3 – Vehicle turning ratio.

Vehicle turning direction	Northern			Eastern			Southern			Western		
	Left	Straight	Right	Left	Straight	Right	Left	Straight	Right	Left	Straight	Right
Ratio (%)	0.15	28.42	71.43	18.15	56.27	25.58	3.16	96.79	0.05	88.59	0.78	10.63

Table 4 – Calibrated parameter values in AIMSUN 7.

Description	Northern	Eastern	Southern	Western
Yellow box speed (km/h)	17	15	15	14
Approaching speed (km/h)	60	60	60	60
Exiting speed (km/h)	60	60	40	60
Visibility distance (m)	10	10	10	15
Presence time (%)	66.8	–	–	72.5

Table 5 presents the AIMSUN result (queuing length) which is average queuing length of 10 replications, showing that the R^2 value of the western and northern approaches are higher than 0.70, and the total queuing lengths for 45 min in the western and northern approaches are also very similar. Although the R^2 of the southern and eastern approaches are less than 0.23, their queuing length is less than 50 m. Therefore, the results of AIMSUN queuing length (western and northern approaches) can be treated as reliable.

4. Queuing length variations with detector location changes

Detector C (305 m) and Detector M (220 m) are currently installed on the Old Belair Road roundabout. For sensitivity tests, both detectors were moved in an incremental of 25 m in the range 180–430 m (Detector C) and 95–345 m (Detector M) in the AIMSUN 7 model. This study then compared the queuing length (45 min) of a total of 121 cases in accordance with the detector location moves as shown in Table 6. When Detector C and Detector M are at 305 m and 220 m respectively, the total queuing length for 45 min reached 9660 m. However, once the detectors were moved to 380 m (Detector C) and 320 m (Detector M), the total queuing length for 45 min was reduced by around 1000 m.

Table 7 lists the queuing length according to the estimated phase normal and red times when Detector C is at 380 m and Detector M is at 320 m, which represents the optimal detector location. With the estimated phase time the total queuing length (western + northern approaches) is 8744 m for 45 min, which only differs by 134 m compared with the AIMSUN results.

Table 5 – Queuing length: drone vs AIMSUN.

Time	Southern		Western		Northern		Eastern	
	Drone (m)	AIMSUN (m)	Drone (m)	AIMSUN (m)	Drone (m)	AIMSUN (m)	Drone (m)	AIMSUN (m)
17:10–17:15	15	14	152	133	770	700	10	35
17:15–17:20	40	14	210	147	720	686	15	35
17:20–17:25	30	28	235	147	880	980	15	42
17:25–17:30	15	28	228	154	1000	1001	0	42
17:30–17:35	30	28	220	273	700	875	7	42
17:35–17:40	45	28	302	322	580	658	7	42
17:40–17:45	40	28	310	336	730	728	10	42
17:45–17:50	45	28	330	357	750	728	7	42
17:50–17:55	30	28	335	490	950	945	0	42
Total	290	224	2297	2359	7080	7301	71	364
R^2	0.0543		0.7676		0.7004		0.2308	

Table 6 – Total queuing length for 45 min (western approach + northern approach).

Northern detector location (m)	Western detector location (m)										
	95	120	145	170	195	220	245	270	295	320	345
180	13,034	12,859	13,118	12,999	12,264	12,369	11,494	10,570	10,563	10,591	10,941
205	11,823	10,794	10,962	10,388	11,207	10,178	8827	9065	8848	8701	9121
230	10,409	11,298	11,074	11,242	10,304	10,269	10,010	9940	10,024	10,010	10,038
255	10,353	13,118	12,173	11,984	10,262	11,333	11,018	11,011	11,011	10,150	9478
280	10,682	10,206	11,991	10,927	12,453	10,591	11,844	11,144	11,060	11,970	11,347
305	10,745	11,872	12,194	12,089	11,900	9660	10,451	10,836	11,767	10,129	10,213
330	10,864	12,208	11,662	12,341	11,347	10,360	11,305	10,423	9961	9940	8855
355	11,620	11,900	11,921	10,640	11,046	10,976	10,521	11,123	9674	9422	9135
380	11,137	10,570	10,752	9737	9653	10,360	9989	10,143	8841	8610	9023
405	12,124	11,186	11,480	10,094	9597	10,269	10,325	10,241	9835	10,220	10,108
430	12,656	10,591	11,102	11,718	10,626	11,144	10,409	10,164	11,396	10,402	11,228

Table 7 – Phase time estimation.

Time	Phase time (s)		Western queuing length (m)		Northern queuing length (m)	
	Green	Red	AIMSUN	Model	AIMSUN	Model
17:10–17:15	240	60	98	138	763	919
17:15–17:20	260	40	133	82	707	695
17:20–17:25	216	84	168	230	819	816
17:25–17:30	195	105	175	296	791	857
17:30–17:35	250	50	252	124	693	591
17:35–17:40	230	70	322	261	546	505
17:40–17:45	190	110	329	386	560	597
17:45–17:50	190	110	336	376	581	632
17:50–17:55	175	125	588	511	749	729
Total	1946	754	2401	2403	6209	6341

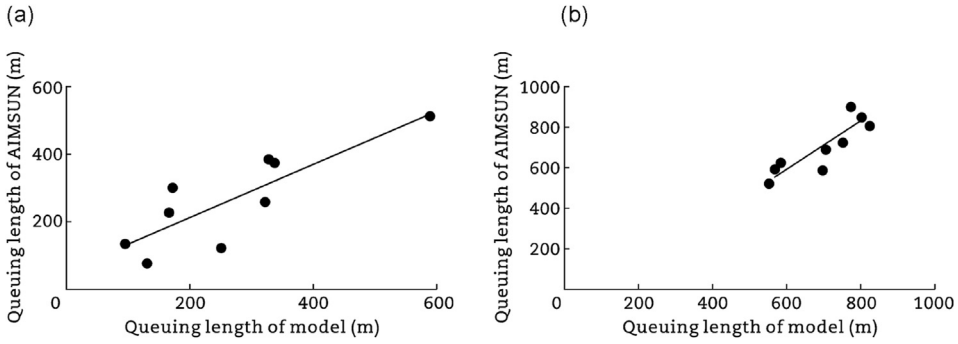

Fig. 8 – Coefficient of determination values. (a) Western approach ($R^2 = 0.712$). (b) Northern approach ($R^2 = 0.725$).

The estimated queuing length was analyzed using the coefficient of determination method, and the R^2 values of both approaches are higher than 0.71 (Fig. 8), therefore, the numerical models demonstrated a robust performance, the queuing length and phase time estimation using the numerical models is possible.

5. Conclusion and future studies

This research formulated numerical models that can be used to estimate vehicle queuing lengths for controlling and metered approaches at signalized metering roundabouts. Calibration and verification simultaneously used drone footage for the measurement of queuing length at two approaches and AIMSUN was applied to test model sensitivities and reliability, when detector location changed.

The modeling results compared to the Old Belair Road roundabout data indicated that the variations of Detectors C and M locations would result the changes of the queuing lengths and phase time splits on the controlling and metered approaches. Although Detectors C's and M's locations are designed at 305 m and 220 m, respectively currently, based on the 121 modeling scenarios, the locations of 380 m (for C) and 320 m (for M) could reduce the queuing length on both approaches.

The R^2 tests demonstrated that the queuing estimation models are capable to evaluate the performance of metering signal roundabouts. Moreover, the numerical models can estimate changes of phase time. Therefore, it can be expected that the numerical models can be used to determine detector locations when a metering roundabout is considered.

However, there are some limitations recognized through this study. First, signal phase time is one of the main variables in estimating queuing length. Although this study adopted two signal phase situations, normal and red, to simplify the analysis process, three signal phases need to be implemented to reflect real signal phases in the future. Second, the constants used in the numerical models have been calibrated for the Old Belair Road roundabout only. In order to achieve more rigorous results, more studies based on additional cases of metering roundabouts should be conducted.

REFERENCES

Afezolli, A., Shehu, E., 2016. The analysis of performance and capacity at a roundabout with metering signals. In: The 3rd International Balkans Conference on Challenges of Civil Engineering, Tirana, 2016.

Akçelik, R., 2004. Roundabouts with unbalanced flow patterns. In: The Institute of Transportation Engineers 2004 Annual Meeting, Lake Buenavista, 2004.

Akçelik, R., 2005. Capacity and performance analysis of roundabout metering signals. In: Transportation Research Board National Roundabout Conference, Vail, 2005.

Akçelik, R., 2006. Analysis of roundabout metering signals. In: The 25th AITPM 2006 National Conference, Melbourne, 2006.

Akçelik, R., 2010. SIDRA Intersection User Guide: Part 4-Output Guide. Akcelik & Associates Pty Ltd., Greythorn.

Akçelik, R., 2011. Roundabout metering signals: capacity, performance and timing. Procedia-Social and Behavioral Sciences 16, 686–696.
Akçelik, R., Chung, E., Besley, M., 1996. Performance of roundabouts under heavy demand conditions. Road and Transport Research 5 (2), 36–57.
Azhar, A.M., Svante, B., 2011. Signal control of roundabouts. Procedia-Social and Behavioral Sciences 16, 729–738.
Chapman, J., Benekohal, R., 2002. Roundabout warrants: proposed framework for future development. Transportation Research Record 1801, 39–45.
Flannery, A., Kharoufeh, J.P., Gautam, N., et al., 2005. Queuing delay models for single-lane roundabouts. Civil Engineering and Environmental Systems 22 (3), 133–150.
Geers, D.G., Tyler, P., Hengst, B., et al., 2009. Enhanced roundabout metering. In: 16th ITS World Congress and Exhibition on Intelligent Transport Systems and Services, Stockholm, 2009.
Guo, R., 2010. Estimating critical gap of roundabouts by different methods. In: Transportation of China, 6th Advanced Forum on Transportation of China, Beijing, 2010.
Hummer, J.E., Milazzo, I., Joseph, S., et al., 2014. The potential for metering to help roundabouts manage peak period demands in the US. In: Transportation Research Board 93rd Annual Meeting, Washington DC, 2014.
Koonce, P., Ringert, J., Urbanik, T., et al., 2002. Detection range setting methodology for signal priority. Journal of Public Transportation 5 (3), 113–136.
Krogscheepers, J., Roebuck, C., 2000. Unbalanced traffic volumes at roundabouts. In: Fourth International Symposium on Highway Capacity, Hawaii, 2000.
Liu, H., Skabardonis, A., Zhang, W.B., et al., 2004. Optimal detector location for bus signal priority. Transportation Research Record 1867, 144–150.
Luttrell, G., Russell, E.R., Rys, M., 2000. Modeling traffic flows through a modern roundabout based on video data. In: Mid-continent Transportation Symposium, Iowa, 2000.
Martin-Gasulla, M., Garcia, A., Moreno, A.T., et al., 2016a. Capacity and operational improvements of metering roundabouts in Spain. Transportation Research Procedia 15, 295–307.
Martin-Gasulla, M., García, A., Moreno, A.T., 2016b. Benefits of metering signals at roundabouts with unbalanced flow: patterns in Spain. Transportation Research Record 2585, 20–28.
Mensah, S., Eshragh, S., Faghri, A., 2010. A critical gap analysis of modern roundabouts. In: Transportation Research Board 89th Annual Meeting, Washington DC, 2010.
Oh, S., Choi, K., 2004. Optimal detector location for estimating link travel speed in urban arterial roads. KSCE Journal of Civil Engineering 8, 327–333.
Robinson, B., Rodegerdts, L., Scarborough, W., et al., 2000. Roundabouts: an Informational Guide. FHWA-RD-00-067. Federal Highway Administration, U.S. Department of Transportation, Washington DC.
Sides, K., 2000. Assessing the clearwater beach entryway roundabout. In: Institute of Transportation Engineers 2000 Annual Meeting and Exhibit, Tennessee, 2000.
Silva, A.B., Santos, S., Gaspar, M., 2013. Turbo-roundabout use and design. In: CITTA 6th Annual Conference on Planning Research, Coimbra, 2013.
Stevens, C.R., 2005. Signals and meters at roundabouts. In: The 2005 Mid-continent Transportation Research Symposium, Ames, 2005.
Sun, X., Ma, W., Huang, W., 2016. Comparative study on the capacity of a signalised roundabout. IET Intelligent Transport Systems 10 (3), 175–185.
Vlahos, E., Polus, A., Lacombe, D., et al., 2008. Evaluating the conversion of all-way stop-controlled intersections into roundabouts. Transportation Research Record 2078, 80–89.
Waddell, E., 1997. Evolution of roundabout technology: a history-based literature review. In: ITE 67th Annual Meeting, Boston, 1997.
Xu, F., Tian, Z.Z., 2008. Driver behavior and gap-acceptance characteristics at roundabouts in California. Transportation Research Record 2071, 117–124.
Zhou, G., Gan, A., Zhu, X., 2006. Determination of optimal detector location for transit signal priority with queue jumper lanes. Transportation Research Record 1978, 123–129.

Hong Ki An is a current PhD researcher at the University of South Australia. He received a bachelor degree of urban/traffic engineering from Dae-Jin University in 2004, then worked at the Korea Transport Institute where he was involved in public transport planning, preliminary feasibility planning and metropolitan transport implementation planning. He received a master's degree from the University of South Australia in 2013 where he is now studying for his PhD degree. His subject is traffic management through the application of metering systems at roundabouts. He has further interests in traffic modeling and public transport systems.

Wen Long Yue. After receiving a bachelor degree of engineering in 1982, Wen Long Yue worked as a consulting engineer involved on projects at feasibility, preliminary and detailed design stages. He then engaged in studies on pedestrian violations at signalized intersections at Wollongong University. From 1989 to 1993, he conducted researches in the development of a parking design and simulation model as his PhD topic at Monash University. Since 1993, he has been working at the University of South Australia. Dr Yue's other research interests include road safety, signalized intersection, public transport systems, transport network and system modeling, fuels for vehicles, and logistics management.

Branko Stazic is a research associate with twenty years of experience as a transportation engineer working for the South Australia's State Government Transport Agency, University of South Australia and the Flinders University in Adelaide. He is currently working for the Flinders Transport Systems and is involved in research, teaching and supervision of students working on transport modeling projects. He holds a master's degree in transport systems engineering from University of South Australia and he is currently undertaking a PhD research degree course at the same university. He has published a number of journal and conference papers on traffic simulation modeling.